ISSN 1001-0742
CN 11-2629/X

JES

JOURNAL OF ENVIRONMENTAL SCIENCES

June 1, 2015 Volume 32
www.jesc.ac.cn

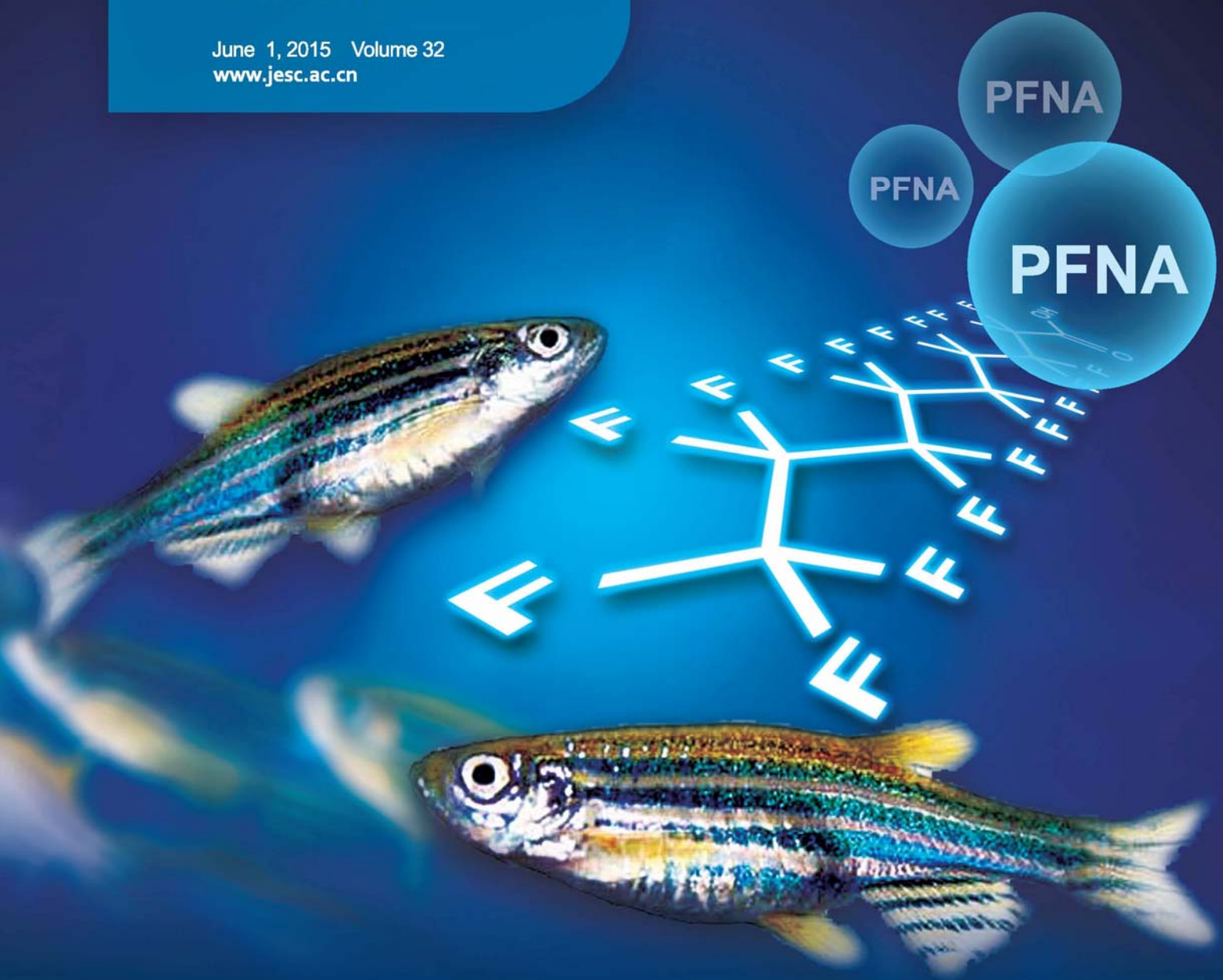

ELSEVIER
Science Press

Sponsored by
Research Center for Eco-Environmental Sciences
Chinese Academy of Sciences

Journal of Environmental Sciences Volume 32 2015

www.jesc.ac.cn

Highlight article

249 Cyanobacterial bloom dynamics in Lake Taihu
Katherine Z. Fu, Birget Moe, Xing-Fang Li and X. Chris Le

Regular articles

1 Membrane fouling controlled by coagulation/adsorption during direct sewage membrane filtration (DSMF) for organic matter concentration
Hui Gong, Zhengyu Jin, Xian Wang and Kaijun Wang

8 Photodegradation of methylmercury in Jialing River of Chongqing, China
Rongguo Sun, Dingyong Wang, Wen Mao, Shibo Zhao and Cheng Zhang

15 Powdered activated carbon adsorption of two fishy odorants in water: Trans,trans-2,4-heptadienal and trans,trans-2,4-decadienal
Xin Li, Jun Wang, Xiaojian Zhang and Chao Chen

26 Toxic effects of perfluorononanoic acid on the development of Zebrafish (*Danio rerio*) embryos
Hui Liu, Nan Sheng, Wei Zhang and Jiayin Dai

35 Denitrification and biofilm growth in a pilot-scale biofilter packed with suspended carriers for biological nitrogen removal from secondary effluent
Yunhong Shi, Guangxue Wu, Nan Wei and Hongying Hu

42 Groundwater arsenic removal by coagulation using ferric(III) sulfate and polyferric sulfate: A comparative and mechanistic study
Jinli Cui, Chuanyong Jing, Dongsheng Che, Jianfeng Zhang and Shuxuan Duan

54 Diurnal and spatial variations of soil NO_x fluxes in the northern steppe of China
Bing Wang, Xinqing Lee, Benny K.G. Theng, Jianzhong Cheng and Fang Yang

62 Effects of elevated atmospheric CO_2 concentration and temperature on the soil profile methane distribution and diffusion in rice-wheat rotation system
Bo Yang, Zhaozhi Chen, Man Zhang, Heng Zhang, Xuhui Zhang, Genxing Pan, Jianwen Zou and Zhengqin Xiong

72 The potential leaching and mobilization of trace elements from FGD-gypsum of a coal-fired power plant under water re-circulation conditions
Patricia Córdoba, Iria Castro, Mercedes Maroto-Valer and Xavier Querol

81 Unraveling the size distributions of surface properties for purple soil and yellow soil
Ying Tang, Hang Li, Xinmin Liu, Hualing Zhu and Rui Tian

90 Prediction of effluent concentration in a wastewater treatment plant using machine learning models
Hong Guo, Kwanho Jeong, Jiyeon Lim, Jeongwon Jo, Young Mo Kim, Jong-pyo Park, Joon Ha Kim and Kyung Hwa Cho

102 Cu-Mn-Ce ternary mixed-oxide catalysts for catalytic combustion of toluene
Hanfeng Lu, Xianxian Kong, Haifeng Huang, Ying Zhou and Yinfei Chen

108 Immobilization of self-assembled pre-dispersed nano-TiO_2 onto montmorillonite and its photo-catalytic activity
Tingting Zhang, Yuan Luo, Bing Jia, Yan Li, Lingling Yuan and Jiang Yu

118 Effects of fluoride on the removal of cadmium and phosphate by aluminum coagulation
Ruiping Liu, Bao Liu, Lijun Zhu, Zan He, Jiawei Ju, Huachun Lan and Huijuan Liu

CONTENTS

126 Structure and function of rhizosphere and non-rhizosphere soil microbial community respond differently to elevated ozone in field-planted wheat
Zhan Chen, Xiaoke Wang and He Shang

135 Chemical looping combustion: A new low-dioxin energy conversion technology
Xiuning Hua and Wei Wang

146 Picoplankton and virioplankton abundance and community structure in Pearl River Estuary and Daya Bay, South China
Zhixin Ni, Xiaoping Huang and Xia Zhang

155 Chemical characterization of size-resolved aerosols in four seasons and hazy days in the megacity Beijing of China
Kang Sun, Xingang Liu, Jianwei Gu, Yunpeng Li, Yu Qu, Junling An, Jingli Wang, Yuanhang Zhang, Min Hu and Fang Zhang

168 Numerical study of the effects of Planetary Boundary Layer structure on the pollutant dispersion within built-up areas
Yucong Miao, Shuhua Liu, Yijia Zheng, Shu Wang, Zhenxin Liu and Bihui Zhang

180 Interaction between Cu^{2+} and different types of surface-modified nanoscale zero-valent iron during their transport in porous media
Haoran Dong, Guangming Zeng, Chang Zhang, Jie Liang, Kito Ahmad, Piao Xu, Xiaoxiao He and Mingyong Lai

189 Tricrystalline TiO_2 with enhanced photocatalytic activity and durability for removing volatile organic compounds from indoor air
Kunyang Chen, Lizhong Zhu and Kun Yang

196 Biogenic volatile organic compound analyses by PTR-TOF-MS: Calibration, humidity effect and reduced electric field dependency
Xiaobing Pang

207 Enhancement of elemental mercury adsorption by silver supported material
Rattabal Khunphonoi, Pummarin Khamdahsag, Siriluk Chiarakorn, Nurak Grisdanurak, Adjana Paerungruang and Somrudee Predapitakkun

217 Characterization of soil fauna under the influence of mercury atmospheric deposition in Atlantic Forest, Rio de Janeiro, Brazil
Andressa Cristhy Buch, Maria Elizabeth Fernandes Correia, Daniel Cabral Teixeira and Emmanoel Vieira Silva-Filho

228 Particle size distribution and characteristics of heavy metals in road-deposited sediments from Beijing Olympic Park
Haiyan Li, Anbang Shi and Xiaoran Zhang

238 Mesoporous carbon adsorbents from melamine–formaldehyde resin using nanocasting technique for CO_2 adsorption
Chitrakshi Goel, Haripada Bhunia and Pramod K. Bajpai

Available online at www.sciencedirect.com

ScienceDirect

www.journals.elsevier.com/journal-of-environmental-sciences

JOURNAL OF ENVIRONMENTAL SCIENCES
www.jesc.ac.cn

Denitrification and biofilm growth in a pilot-scale biofilter packed with suspended carriers for biological nitrogen removal from secondary effluent

Yunhong Shi, Guangxue Wu, Nan Wei, Hongying Hu*

Key Laboratory of Microorganism Application and Risk Control (MARC) of Shenzhen, Graduate School at Shenzhen, Tsinghua University, Shenzhen 518055, China. E-mail: shiyunhong1991@126.com

ARTICLE INFO

Article history:
Received 9 August 2014
Revised 10 December 2014
Accepted 16 December 2014
Available online 2 April 2015

Keywords:
Tertiary denitrification
Pilot-scale biofilter
Biokinetics
Suspended carriers
Biofilm

ABSTRACT

Tertiary denitrification is an effective method for nitrogen removal from wastewater. A pilot-scale biofilter packed with suspended carriers was operated for tertiary denitrification with ethanol as the organic carbon source. Long-term performance, biokinetics of denitrification and biofilm growth were evaluated under filtration velocities of 6, 10 and 14 m/hr. The pilot-scale biofilter removed nitrate from the secondary effluent effectively, and the nitrate nitrogen (NO_3-N) removal percentage was 82%, 78% and 55% at the filtration velocities of 6, 10 and 14 m/hr, respectively. At the filtration velocities of 6 and 10 m/hr, the nitrate removal loading rate increased with increasing influent nitrate loading rates, while at the filtration velocity of 14 m/hr, the removal loading rate and the influent loading rate were uncorrelated. During denitrification, the ratio of consumed chemical oxygen demand to removed NO_3-N was 3.99–4.52 mg/mg. Under the filtration velocities of 6, 10 and 14 m/hr, the maximum denitrification rate was 3.12, 4.86 and 4.42 g N/(m^2·day), the half-saturation constant was 2.61, 1.05 and 1.17 mg/L, and the half-order coefficient was 0.22, 0.32 and 0.24 $(mg/L)^{1/2}$/min, respectively. The biofilm biomass increased with increasing filtration velocity and was 2845, 5124 and 7324 mg VSS/m^2 at filtration velocities of 6, 10 and 14 m/hr, respectively. The highest biofilm density was 44 mg/cm^3 at the filtration velocity of 14 m/hr. Due to the low influent loading rate, biofilm biomass and thickness were lowest at the filtration velocity of 6 m/hr.

Introduction

Conventional secondary effluent in wastewater treatment plants containing high concentrations of nitrate and nitrogen is one of the limiting factors inducing eutrophication in receiving water bodies. Tertiary denitrification of the secondary effluent is an effective method for nitrate removal to control the eutrophication of receiving water bodies (Boltz et al., 2012). During denitrification, oxidized nitrogen is denitrified to nitrogen gas under anoxic conditions, with organic carbon as the electron donor. However, the amount of biodegradable organic carbon in the secondary effluent is limited. Therefore, external organic carbon should be supplied for tertiary denitrification, and commonly used sources include methanol, ethanol and glucose (Park et al., 2009). Compared with other external carbon sources, denitrification with ethanol has several advantages as follows: (1) short acclimation duration (Nyberg et al., 1996), (2) high denitrification rate (Taljemark et al., 2004; Welander and Mattiasson, 2003), (3) less affected by temperature (Mokhayeri et al., 2006), and (4) less harmful to the environment.

* *Corresponding author*. E-mail: wu.guangxue@sz.tsinghua.edu.cn (Guangxue Wu).

http://dx.doi.org/10.1016/j.jes.2014.12.012

High-density carriers such as quartz and ceramic sands have been often used as the media for tertiary denitrification (de Barbadillo et al., 2006), while few studies have focused on biofilters with suspended carriers. The main drawback of biofilters with high-density carriers includes high head loss and high energy requirement for backwashing, while the effluent from biofilters with suspended carriers often contains a high concentration of suspended solids (SS), and additional processes are required to remove SS. For example, in the South Caboolture Water Reclamation Plant, a moving bed biofilm reactor (MBBR) with suspended carriers was shown to be able to reduce nitrate to below 1 mg/L, and filtration was subsequently carried out to remove SS (Wilson et al., 2008). In order to remove oxidized nitrogen and SS simultaneously, a new type of biofilter packed with composite suspended and sand carriers was designed for post-denitrification of secondary effluent, and the lab-scale system could remove nitrate and SS efficiently (Shi et al., 2014).

Filtration velocity affects the kinetics of denitrification and biofilm growth, and consequently affects the system performance of the biofilter. At low filtration velocity, a long reaction duration will be required to metabolize pollutants thoroughly, and in addition, due to the low influent loading rate, a biomass-limited condition often exists. At high filtration velocity, the reaction duration is short and denitrification may be inadequate, and the biofilm will be thin with high shear stress. Wei et al. (2014) found that the denitrification rate increased with increasing filtration velocity. In a denitrifying biofilm system, biomass, density and thickness of biofilm affect the substrate conversion rate, thus affecting the denitrification efficiency. For example, in an aerobic biofilm reactor, the penetration depth of oxygen in the biofilm is in general 100–150 μm, therefore, for maximizing aerobically biological processes, the biofilm thickness should not exceed about 150 μm (Tijhuis et al., 1994). The thickness of the biofilm is determined by balancing growth and detachment of biofilm biomass. The substrate loading rate affects the growth of the biofilm directly, and a high substrate loading rate leads to a high amount of biomass and a thick biofilm (Tijhuis et al., 1994). The detachment of biofilm is affected by hydrodynamic conditions, backwashing frequency and the filling ratio of carriers. Neethling et al. (2010) found that a balance existed between the backwashing frequency and the appropriate thickness of biofilm. Melo and Vieira (1999) found that the biofilm density increased with increasing flow rate, and the biofilm density ranged between 14 and 28 mg/cm^3. Wäsche et al. (2002) showed that the biofilm density increased with increasing sheer stress and substrate load rates, and the biofilm density ranged between 10 and 65 mg/cm^3. To date, studies on the biokinetics of denitrification and biofilm growth for tertiary biofilm systems have been relatively few, and further investigations are required.

A pilot-scale biofilter packed with composite suspended and sand carriers was operated under filtration velocities of 6, 10 and 14 m/hr (corresponding to empty bed retention times (EBRTs) of 17.8, 10.7 and 7.6 min, respectively) with ethanol as the organic carbon source. Long-term performance of the system and denitrifying kinetics were investigated so as to clarify the denitrification performance for the removal of nitrogen. In addition, biofilm growth was measured so as to correlate it with denitrifying performance.

1. Materials and methods

1.1. Pilot-scale biofilter and its operation

The schematic diagram of the experimental biofilter is shown in Fig. 1. The pilot-scale biofilter was made from a plexiglass column with a diameter of 20 cm and a height of 300 cm, and its effective volume was 91 L. The packed height of suspended carriers (specific surface area of 500 m^2/m^3, SPR-1 type, Spring, Qingdao, China) was 178 cm. Sampling ports were provided at different heights along the biofilter. There was a pre-mixing zone with a height of 12 cm on the top of the reactor to facilitate the mixing of the secondary effluent and the organic carbon. At the bottom of the biofilter, there was a support gravel stone layer of 10 cm and a quartz sand layer of 20 cm with sizes between 2 and 4 mm for the removal of SS.

The secondary effluent in the 7th Wastewater Treatment Plant, Kunming, China, was used as the feed. During the study, the influent chemical oxygen demand (COD) concentration was 20 mg/L, nitrate nitrogen (NO_3-N) was 11.2 mg/L, ortho-phosphate (PO_4-P) was 0.45 mg/L, nitrite nitrogen (NO_2-N) was 0.25 mg/L, pH was 6.9 and dissolved oxygen (DO) was 2.4 mg/L.

During operation, the external carbon dosage was 5.4 g COD/g NO_3-N. The treated wastewater and ethanol were fed *via* peristaltic pumps from the top of the biofilter. The filtration velocity was controlled by the speed of the peristaltic pump. The biofilter was backwashed every 24 hr for 15 min with combined air and water. During backwashing, the water flow rate was 10 L/(m^2·sec) and the air flow rate was 5 L/(m^2·sec). During the start-up period, the filtration velocity was 6 m/hr, and after the system reached steady state and adequate data were collected, it was then increased to 10 and 14 m/hr sequentially.

1.2. Batch experiments

Long-term performance, denitrifying biokinetics of backwashed biofilm biomass and biofilm biomass on suspended carriers, and characteristics of biofilm were tested under the filtration velocities of 6, 10 and 14 m/hr, respectively.

During the long-term operation, parameters such as COD, NO_3-N, NO_2-N, ammonium nitrogen (NH_4-N), pH and DO were tested daily to examine the dynamics of nutrient removal in the biofilter.

Under steady state at each filtration velocity, samples were taken at 0, 23, 53, 88, 118, 148, 178, 208, 238 and 278 cm along the biofilter depth, and concentrations of typical parameters (NO_3-N, NO_2-N, COD, DO and pH) were tested so as to investigate the denitrifying biokinetics of the biofilter. At different stages of the experiment, 2 L of backwashed biofilm biomass was taken for batch experiments. Potassium nitrate and ethanol were dosed to achieve the initial NO_3-N and COD of 30 mg/L and 200 mg/L, respectively. After the beginning of the batch experiment, samples were taken at 5 min intervals. The samples were centrifuged at 12,000 r/min for 2 min, and then the supernatant was stored at 4°C for further analysis of NO_3-N, NO_2-N and COD.

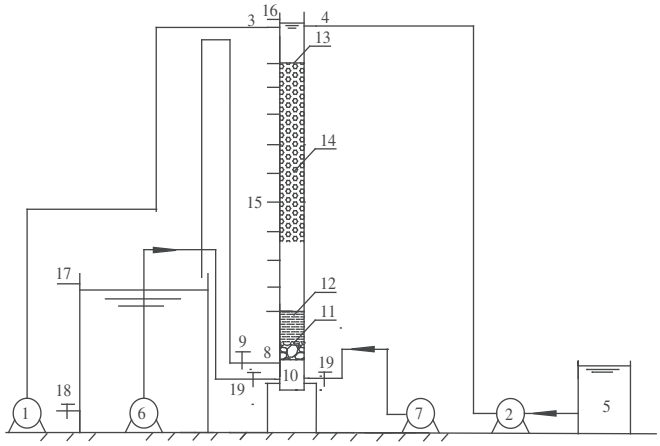

Fig. 1 – Schematic diagram of the pilot-scale biofilter. (1): influent pump; (2): external carbon dosing pump; (3): influent port; (4): external carbon port; (5): external carbon stock tank; (6): backwashing water pump; (7): backwashing air pump; (8): effluent; (9): effluent valve; (10): effluent storage; (11): gravel stone layer; (12): quartz sand layer; (13): perforated plate; (14): suspended carriers; (15): water sampling port; (16): backwashing effluent; (17): effluent; (18): drain valve; (19): check valve; (20): controller.

During the experiment, suspended carriers were taken from the biofilter regularly, and biofilm biomass, thickness and density were measured.

1.3. Analytical methods

COD, NO_3-N, NO_2-N, NH_4-N, PO_4-P, SS and volatile suspended solids (VSS) were tested according to standard methods (APHA, 1999). The pH, DO and NTU were measured using probes pH3110 (WTW, Germany), OXI315i (WTW, Germany) and 1900C (HACH, USA), respectively.

To measure the biofilm biomass, four pieces of media with biofilm were taken from the biofilter. The biomass was washed off from the suspended carriers with distilled water and VSS was determined. The thickness and density of the biofilm were calculated based on Eqs. (1)–(3) (Shrestha et al., 2009; Alves et al., 2002):

$$W = \frac{VSS}{A} \tag{1}$$

$$\rho = \frac{W}{V} \tag{2}$$

$$L = \frac{W}{\rho} \tag{3}$$

where W (g/m^2) is the biofilm biomass on the specific surface area, VSS (g) is the volatile weight of biofilm biomass, A (m^2) is the biofilm surface area, ρ (g/m^3)is the biofilm density, V (m^3/m^2) is the average volume of the wet biofilm on the specific surface area, and L (m) is the biofilm thickness.

Denitrification rates were obtained by fitting the dynamics of oxidized nitrogen with linear equations. According to the Monod equation (Eq. (4)), the half-saturation constant was obtained by AQUASIM using the maximum denitrification rate (Reichert, 1994; Fenu et al., 2010).

$$R = \frac{R_{max} * S}{K_S + S} \tag{4}$$

where R (mg/(L·min)) is the denitrification rate, R_{max} (mg/(L·min)) is the maximum denitrification rate, S (mg/L) is the nitrate concentration, and K_s (mg/L) is the half saturation coefficient for nitrate.

The denitrification process in the biofilter could be described with a half-order reaction as follows (Harremoes, 1976):

$$C = C_i\left(1-\frac{1}{2}\frac{K_{1/2v}}{C_i^{1/2}}\frac{Ha}{Q}\right)^{1/2} \tag{5}$$

where C (mg/L) is the nitrate concentration at different biofilm depths, C_i (mg/L) is the initial nitrate concentration, $K_{1/2v}$ ((mg/L)$^{1/2}$/min) is the half-order coefficient, H (dm) is the biofilter depth from the inlet, a (dm^2) is the area of biofilter and Q (L/min) is the flow rate.

2. Results and discussion

2.1. Long-term performance

The dynamics of nitrate for the biofilter during the 70 days of long-term operation is shown in Fig. 2. The biofilter reached steady state after 11 days of operation. For the influent NO_3-N concentration of 12.4 mg/L, the effluent NO_3-N concentration was 1.3 mg/L. During the start-up period, the water temperature was 19°C. de Barbadillo et al. (2008) found that with acetate as the organic carbon source, the biofilter reached steady state after 3 days of operation with the influent NO_3-N concentration of 10 mg/L at 15°C. By using ethanol as the organic carbon source, Shi et al. (2014) operated the biofilter system with the influent NO_3-N concentration of 10–15 mg/L and the acclimation time was 5 days. Compared with previous studies, the start-up period in this study was slightly long. The possible reason could be due to the low influent nitrate concentration (5.86 mg/L) during the initial stage of the start-up period, and the relatively low substrate

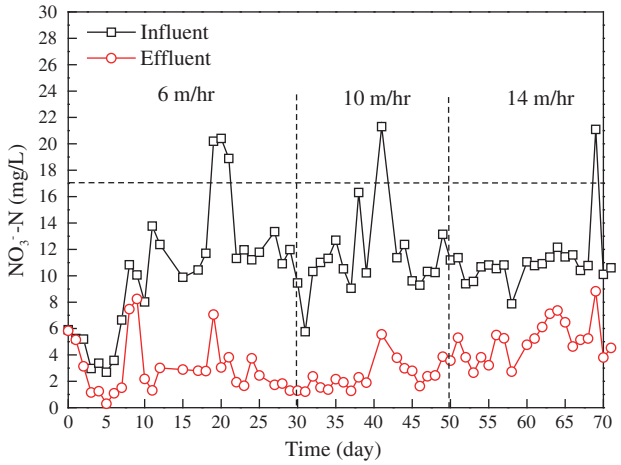

Fig. 2 – Dynamics of NO_3-N under different filtration velocities.

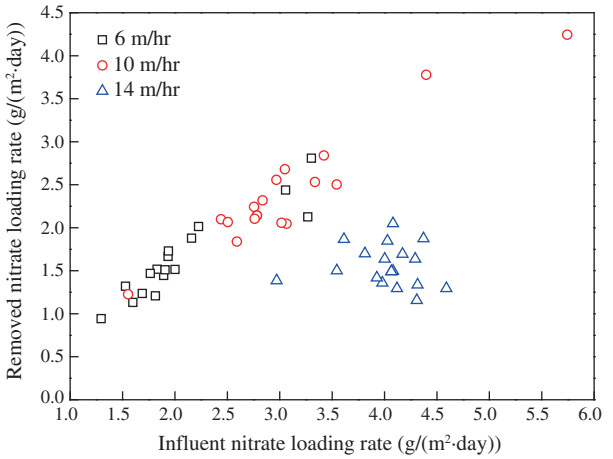

Fig. 3 – Relationship between the NO_3-N removal loading rate and the influent NO_3-N loading rate.

loading rate that limited the growth of biofilm (Stinson et al., 2009).

At the filtration velocities of 6, 10 and 14 m/hr, the influent NO_3-N concentration was 13.1 ± 3.4, 11.5 ± 3.2 and 11.2 ± 2.5 mg/L and the effluent NO_3-N concentration was 2.7 ± 1.4, 2.6 ± 1.1 and 5.1 ± 1.5 mg/L, with the corresponding removal percentage of 82%, 78% and 55%, respectively. By using the MBBR system to enhance denitrification with ethanol as the organic carbon source, Taljemark et al. (2004) also obtained similar results, and the NO_3-N removal percentage was 51% with a filling ratio of suspended carriers of 36% and EBRT of 40–100 min. The influent COD concentration was 93, 97 and 79 mg/L and the effluent COD concentration was 44, 41 and 49 mg/L, with the corresponding removal percentage of 64%, 57% and 37%, respectively. By calculation, during denitrification, the ratio of consumed COD to removed NO_3-N was 4.34, 4.52 and 3.99 mg COD/mg NO_3-N. The results were similar to those obtained in previous studies. For example, by operating a biofilter system, ÆsØy et al. (1998) obtained a value of 4–5 mg COD/mg NO_X-N with ethanol as the organic carbon source, and de Barbadillo et al. (2008) found that the carbon requirement was 5.2 mg COD/mg NO_X-N with ethanol.

The relationship between the influent nitrate loading rate and the nitrate removal loading rate is shown in Fig. 3. At the filtration velocities of 6, 10 and 14 m/hr, the average influent nitrate loading rates were 2.07, 3.09 and 4.06 g N/(m^2·day), respectively. The average nitrate removal loading rates were 1.64, 2.41 and 1.47 g N/(m^2·day). Based on the small-scale system, at the EBRT of 30 min, Bill et al. (2009) obtained a removal loading rate of 0.9 g NO_X-N/(m^2·day) with the influent loading rate of 1.9 g NO_X-N/(m^2·day) and ethanol as the organic carbon source. By operating a MBBR to treat low loading wastewater, Wilson et al. (2008) found that the maximum removed loading rate was 0.58 g N/(m^2·day), with methanol as the organic carbon source and the influent nitrate loading rate of 0.1–0.75 g N/(m^2·day). The main reason for the high nitrate removal loading rate was due to the fact that the influent loading rate was high. During denitrification, the nitrate removal loading rate was correlated with the influent loading rate and increased with increasing influent loading rates generally (Koch and Siegrist, 1997). At filtration velocities of 6 and 10 m/hr, the nitrate removal loading rate increased with increasing influent loading rates, while at the filtration velocity of 14 m/hr, there was no obvious relationship between the influent loading rate and the removal loading rate. Holloway et al. (2008) and Wilson et al. (2008) also obtained similar trends. Within a certain range of influent nitrate loading rates, the removal loading rate increased with increasing influent loading rates. However, when the influent loading rate was above a certain value, the removal capacity reached the maximum and the removal loading rate could not be increased. The main reason for this tendency might be due to the presence of different limiting factors. Considering the loading rate of nitrate from the viewpoint of the substrate or biomass relationship, under filtration velocities of 6 and 10 m/hr, the system might be limited by the substrate, while at the filtration velocity of 14 m/hr, the denitrification might be limited by the biofilm biomass. This might be the reason for the different results obtained for the relationship for different loading rates.

2.2. Denitrifying kinetics of biofilter

The dynamics of nitrogen for the biofilter and backwashed biofilm biomass are shown in Fig. 4.

Under different filtration velocities, denitrification occurred within all the biofilter depths. At the filtration velocities of 6, 10 and 14 m/hr, NO_2-N accumulation was not obvious, and the denitrifying rate was considered to be equal to the NO_3-N removal rate, with values of 23.0, 17.1, 11.7 mg/(g VSS·hr), respectively. For denitrification of the backwashed biofilm biomass, accumulation of NO_2-N was obvious. At the filtration velocities of 6, 10 and 14 m/hr, the highest NO_2-N concentration was 6.12, 2.69 and 5.61 mg/L, respectively. During denitrification, the NO_2-N denitrifying rate could be obtained by subtracting the NO_2-N accumulation rate from the NO_3-N removal rate. At the filtration velocities of 6, 10 and 14 m/hr, the NO_3-N removal rate was 44.6, 64.8 and 61.8 mg/(g VSS · hr) and the NO_2-N denitrifying rate was 21.5, 49.2 and 39.3 mg/(g VSS·hr), respectively. Therefore, the reason for NO_2-N accumulation was that the NO_3-N removal rate

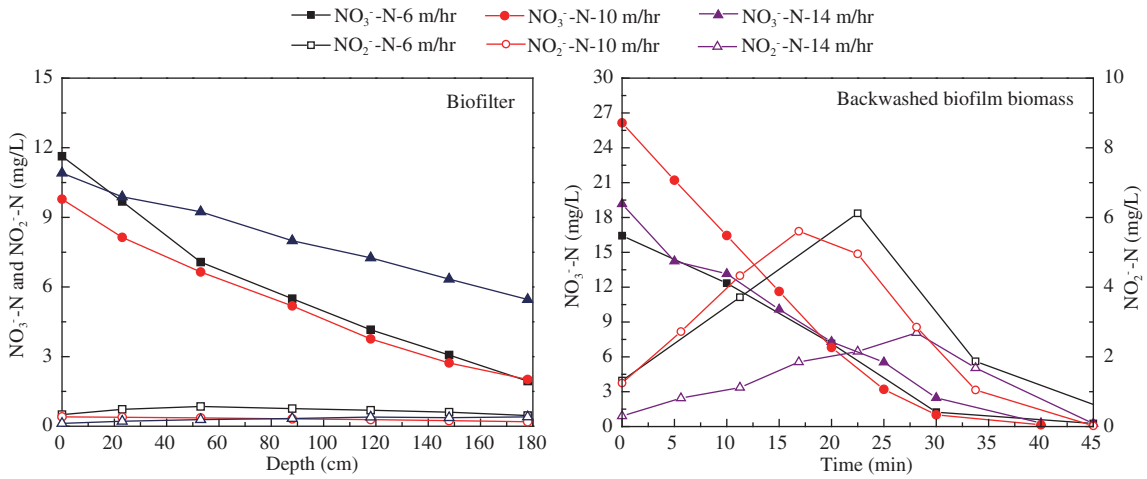

Fig. 4 – Dynamics of NO_3-N and NO_2-N during denitrification for both biofilter biomass and the backwashed biofilm biomass.

was higher than the NO_2-N denitrifying rate. The NO_3-N removal rate of the backwashed biofilm biomass was much higher than that within the biofilter, which might be due to lower substrate diffusion within the biofilm (possibly caused by the density and thickness of biofilm).

According to the Monod equation (Eq. (4)), when S is far above K_s, R equals R_{max}. An external carbon source possessing high R_{max} and low K_s is most desirable. Shrestha et al. (2009) and Bill et al. (2009) found that the K_s value was low, suggesting low mass transfer resistance. Under the filtration velocities of 6, 10 and 14 m/hr, the maximum denitrification rates were 3.12, 4.86 and 4.42 g N/(m^2·day), and the half-saturation constants were 2.61, 1.05 and 1.17 mg/L, respectively. By operating the MBBR system with ethanol as the organic carbon source, Bill et al. (2009) obtained a maximum denitrification rate and half-saturation constant of 2.2 g N/(m^2·day) and 2.2 mg/L, respectively. With methanol as the organic carbon source and water temperature of 12.5–20°C, Shrestha et al. (2009) found that the K_s increased with increasing biomass within the range of 0.6–1.1 mg/L. In a MBBR system, Peric et al. (2009b) found that the maximum denitrification rates and the half-saturation constants were 3.1 g N/(m^2·day) and 2.5 mg/L at 17°C and 3.05 g N/(m^2·day) and 2.4 mg/L at 13.5°C. The study of Peric et al. (2009b) indicated that K_s was not affected by temperature and biofilm thickness. At the filtration velocities of 10 and 14 m/hr, K_s was lower than that at the filtration velocity of 6 m/hr, while the biofilm thickness was higher than that at the filtration velocity of 6 m/hr. Therefore, biofilm thickness and K_s were not directly correlated.

Under different filtration velocities, good linear relationships between the half-order NO_3-N concentration and the EBRT were obtained, and the half-order coefficients were 0.22, 0.32 and 0.24 $(mg/L)^{1/2}$/min, respectively. At the EBRT of 30 min, Janning et al. (1995) found that the half-order coefficient was 0.21 and 0.18 $(mg/L)^{1/2}$/min with the influent half-order NO_3-N concentration of 4–4.5 $(mg/L)^{1/2}$ and 2.5–3 $(mg/L)^{1/2}$, respectively. Harremoes (1976) found that the half-order coefficient was 0.305 $(mg/L)^{1/2}$/min with the influent NO_3-N concentration of 15.2 mg/L and the EBRT of 15 min. The main reason for the maximum half-order coefficient obtained at the filtration velocity of 10 m/hr might be the good hydraulic conditions and adequate reaction duration obtained under this condition. At the filtration velocity of 14 m/hr, the half-order coefficient was significantly lower than that at the filtration rate of 10 m/hr. This might be due to the fact that at the filtration velocity of 14 m/hr, the EBRT of only 7.6 min limited denitrification due to biomass limitation rather than substrate limitation.

2.3. Characteristics of biofilm growth

Biofilm biomass and thickness in the biofilter during the 70 days of long-term operation are shown in Fig. 5, and the average values under each filtration velocity are shown in Table 1.

The biofilm biomass increased with increasing filtration velocity. The main reason for the different biomass at different filtration velocities was that the influent substrate loading rate increased with increasing filtration velocity. Generally, under the same operation conditions, the higher the nutrient concentration and the loading rate, the higher the biomass amount (ÆsØy et al., 1998). Stinson et al. (2009) found that the amount of biomass was low in the MBBR system with low influent NO_3-N concentrations. With a filling ratio of suspended carriers of 30% and influent loading rate of 1.43–2.13 g N/(m^2·day) at 11.1–17°C, Stinson et al. (2009) found that the biomass on the suspended carriers was 12–22 g SS/m^2. Compared with previous studies, the biofilm biomass in this study was relatively low. The possible reasons could be as follows. (1) During the experiment, the temperature was relatively high at 22°C. Shrestha et al. (2009) and Peric et al. (2009a) found that the amount of biomass increased with decreasing temperatures. Thick and high amount of biofilm was formed at low temperatures (Welander and Mattiasson, 2003). (2) In this study, the backwashing frequency was once a day and some biofilm was detached during backwashing. ÆsØy et al. (1998) showed that the backwashing frequency had a significant impact on the biofilm biomass. (3) The filling ratio of suspended carriers was 64% in this study. Duan et al. (2013) found that a high media fill ratio could increase the chance of biofilm detachment from the media.

Both biofilm density and thickness were different under different filtration velocities. At the filtration velocity of

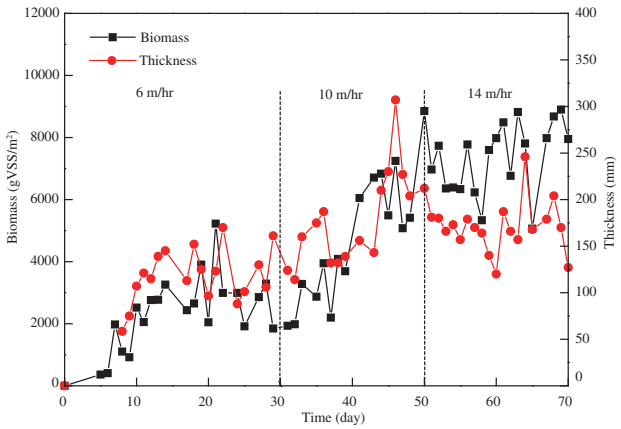

Fig. 5 – Dynamics of biofilm biomass and thickness under different filtration velocities.

14 m/hr, the biofilm density was 44 mg/cm^3, which was much higher than those at the filtration velocities of 6 and 10 m/hr. The biofilm density increased with increasing sheer stress. Under the same operating conditions, the sheer stress was high at the filtration velocity of 14 m/hr. Kwok et al. (1998) and Melo and Vieira (1999) also obtained similar results. At the filtration velocity of 6 m/hr, the biofilm thickness was thinnest. The reason was that the influent substrate loading rate was low at the filtration velocity of 6 m/hr. By operating a fluidized bed biofilm reactor with the temperature of 26–30°C and the hydraulic retention time of 1 hr, Alves et al. (2002) found that the density and thickness of biofilm were 5–15 mg/cm^3 and 344–402 μm, respectively. Tijhuis et al. (1994) found that there was competition for substrate between suspended and attached biomass in the biofilm system. Due to the substrate diffusion limitation, the attached biomass possessed weak competitiveness. Compared with previous studies, the biofilm was dense and thin in this study. This might be due to the fact that the amount of suspended biomass was low and the substrate was adequate for the growth of biofilm within low EBRTs (7.6–17.8 min).

The performance of the biofilter system was dependent on both the kinetics of denitrification and biofilm growth. At low filtration velocities, the denitrification process was complete with sufficient residence time, but the amount of biomass was less due to the low influent substrate loading rate. At high filtration velocities, the biofilm was thin due to the high sheer stress, which was good for substrate diffusion, but the contact time between biomass and substrate was inadequate. It is necessary to balance the kinetics of denitrification and biofilm growth by controlling filtration velocity in a suitable range.

Table 1 – Biomass, density and thickness of biofilm at different filtration velocities.

Filtration velocity (m/hr)	Biofilm biomass (mg VSS/m^2)	Biofilm density (mg/cm^3)	Biofilm thickness (μm)
6	2845	23.46	125
10	5124	27.76	187
14	7324	44.09	170

3. Conclusions

(1) The biofilter reached steady state after 11 days of operation. Under the filtration velocities of 6, 10 and 14 m/hr, the NO_3-N removal percentage was 82%, 78% and 55%, respectively. During denitrification, the ratio of consumed COD to removed NO_3-N was 4.34, 4.52 and 3.99 mg/mg.(2) The denitrification rate of backwashed biofilm biomass was similar under different filtration velocities. The different denitrification rates found for the biofilter were due to different biofilm structures. Under the filtration velocities of 6, 10 and 14 m/hr, the maximum denitrification rates were 3.12, 4.86 and 4.42 g N/(m^2·day), the half-saturation constants were 2.61, 1.05 and 1.17 mg/L, and the half-order coefficients were 0.22, 0.32 and 0.24 (mg/L)$^{1/2}$/min, respectively. At the filtration velocity of 10 m/hr, the half-order coefficient was largest and the half-saturation constant was lowest. (3) The biofilm biomass increased with increasing filtration velocity and was 2845, 5124, 7324 mg VSS/m^2 at the filtration velocities of 6, 10 and 14 m/hr, respectively. The biofilm density was 23.46, 27.76 and 44.09 mg/cm^3, and the biofilm thickness was 125, 187 and 170 μm, respectively. The density of biofilm was highest at the filtration velocity of 14 m/hr due to high sheer stress. At the filtration velocity of 6 m/hr, the biofilm thickness was lowest.

Acknowledgments

This research was supported by the Major Science and Technology Program for Water Pollution Control and Treatment of China (No. 2012ZX07302002).

REFERENCES

Æsøy, A., Ødegaard, H., Bach, K., 1998. Denitrification in a packed bed biofilm reactor (BIOFOR)—experiments with different carbon sources. Water Res. 32 (5), 1463–1470.

Alves, C.F., Melo, L.F., Vieira, M.J., 2002. Influence of medium composition on the characteristics of a denitrifying biofilm formed by *Alcaligenes denitrificans* in a fluidised bed reactor. Process Biochem. 37 (8), 837–845.

APHA (American Public Health Association), AWWA (American Water Works Association), WEF (Water Environment Federation), 1999. Standard Methods for the Examination of Water and Wastewater. 20th ed. (Washington DC, USA).

Bill, K.A., Bott, C.B., Murthy, S.N., 2009. Evaluation of alternative electron donors for denitrifying moving bed biofilm reactors (MBBRs). Water Sci. Technol. 60 (10), 2647–2657.

Boltz, J.P., Morgenroth, E., Daigger, G.T., Debarbadillo, C., Murthy, S., Sørensen, K.H., et al., 2012. Method to identify potential phosphorus rate-limiting conditions in post-denitrification biofilm reactors within systems designed for simultaneous low-level effluent nitrogen and phosphorus concentrations. Water Res. 46 (19), 6228–6238.

de Barbadillo, C., Rectanus, R., Canham, R., 2006. Tertiary denitrification and very low phosphorus limits: a practical look at phosphorus limitations on denitrification filters. Proceedings of the Water Environment Federation, WEFTEC 2006. Texas, USA. Oct. 21–25.

de Barbadillo, C., Miller, P., Ledwell, S., 2008. A comparison of operating issues and dosing requirements for alternative

carbon sources in denitrification filters. Proceedings of the Water Environment Federation, WEFTEC 2008. Chicago, USA. Oct. 18–22.
Duan, L., Jiang, W., Song, Y.H., Xia, S.Q., Hermanowicz, S.W., 2013. The characteristics of extracellular polymeric substances and soluble microbial products in moving bed biofilm reactor-membrane bioreactor. Bioresour. Technol. 148, 436–442.
Fenu, A., Guglielmi, G., Jimenez, J., Sperandio, M., Saroj, D., 2010. Activated sludge model (ASM) based modelling of membrane bioreactor (MBR) processes: a critical review with special regard to MBR specificities. Water Res. 44 (15), 4272–4294.
Harremoes, P., 1976. The significance of pore diffusion to filter denitrification. J. Water Pollut. Control Fed. 48 (2), 377–388.
Holloway, R., Zhao, H., Rinne, T., Thesing, G., Parker, J., Beals, M., 2008. The impact of temperature and loading on meeting stringent nitrogen requirements in a two-stage BAF—a comparison of pilot and full-scale performance. Proceedings of the Water Environment Federation, WEFTEC 2008. Chicago, USA. Oct. 18–22.
Janning, K.F., Harremoes, P., Nielsen, M., 1995. Evaluating and modelling the kinetics in a full scale submerged denitrification filter. Water Sci. Technol. 32 (8), 115–123.
Koch, G., Siegrist, H., 1997. Denitrification with methanol in tertiary filtration at wastewater treatment plant Zürich-Werdhoölzli. Water Sci. Technol. 36 (1), 165–172.
Kwok, W.K., Picioreanu, C., Ong, S.L., van Loosdrecht, M.C.M., Ng, W.J., Heijnen, J.J., 1998. Influence of biomass production and detachment forces on biofilm structures in a biofilm airlift suspension reactor. Biotechnol. Bioeng. 58, 400–407.
Melo, L.F., Vieira, M.J., 1999. Physical stability and biological activity of biofilms under turbulent flow and low substrate concentration. Bioprocess Eng. 20 (4), 363–368.
Mokhayeri, Y., Nichols, A., Murthy, S., 2006. Examining the influence of substrates and temperature on maximum specific growth rate of denitrifiers. Water Sci. Technol. 54 (8), 155–162.
Neethling, J.B., de Barbadillo, C., Falk, M., Liu, H.-Y., 2010. Tertiary denitrification processes for low nitrogen and phosphorus. Available at https://http://www.werf.org/c/KnowledgeAreas/NutrientRemoval/compendium/05-Tertiary_Denitrification_Processes.aspx.
Nyberg, U., Andersson, B., Aspegren, H., 1996. Long-term experiences with external carbon sources for nitrogen removal. Water Sci. Technol. 33 (12), 109–116.
Park, J.B.K., Craggs, R.J., Sukias, J.P.S., 2009. Removal of nitrate and phosphorus from hydroponic wastewater using a hybrid denitrification filter (HDF). Bioresour. Technol. 100 (13), 3175–3179.
Peric, M., Neupane, D., Stinson, B., 2009a. Phosphorous requirements in a post denitrification MBBR at a combined limit of technology nitrogen and phosphorous plant. Proceedings of the Water Environment Federation, Nutrient Removal 2009. Washington, DC, USA. Jun. 28–Jul. 1.
Peric, M., Stinson, B., Neupane, D., Kharkar, K., Mokhayeri, Y., Carr, J., et al., 2009b. Kinetic/half-saturation coefficient considerations for post denitrification MBBR. Proceedings of the Water Environment Federation, WEFTEC 2009. Florida, USA. Oct. 10–14.
Reichert, P., 1994. AQUASIM—a tool for simulation and data analysis of aquatic systems. Water Sci. Technol. 30 (2), 21–30.
Shi, Y., Wei, N., Wu, G., Hu, H., 2014. Post-denitrification of the secondary effluent in biofilters packed with composite carriers. Proceedings of the IWA Workshop on Resource Recovery from Wastewater/Bio-Solids. Harbin, China. Jul. 13–15.
Shrestha, A., Riffat, R., Bott, C., Takacs, C., Stinson, I., 2009. Denitrification stoichiometry and kinetics of moving bed biofilm reactor. Proceedings of the Water Environment Federation, Nutrient Removal 2009. Washington, DC, USA. Jun. 28–Jul. 1.
Stinson, B., Peric, M., Neupane, D., Laquidara, M., Locke, E., Murthy, S., et al., 2009. Design and operating considerations for a post denitrification MBBR to achieve limit of technology effluent NOx 1 mg/l and effluent TP 0.18 mg/l. Proceedings of the Water Environment Federation, WEFTEC 2009. Florida, USA. Oct. 10–14.
Taljemark, K., Aspegren, H., Gruvberger, C., Hanner, N., Nyberg, U., Andersson, B., 2004. 10 Years of experiences of an MBBR process for post-denitrification. Proceedings of the Water Environment Federation, WEFTEC 2004. Louisiana, USA. Oct. 2–6.
Tijhuis, L., Van Loosdrecht, M.C.M., Heijnen, J.J., 1994. Formation and growth of heterotrophic aerobic biofilms on small suspended particles in airlift reactors. Biotechnol. Bioeng. 44 (5), 595–608.
Wäsche, S., Horn, H., Hempel, D.C., 2002. Influence of growth conditions on biofilm development and mass transfer at the bulk/biofilm interface. Water Res. 36 (19), 4775–4784.
Wei, N., Shi, Y.H., Wu, G.X., Hu, H.Y., Wu, Y.H., Wen, H., 2014. Tertiary denitrification of the secondary effluent by denitrifying biofilters packed with different sizes of quartz sand. Water 6 (5), 1300–1311.
Welander, U., Mattiasson, B., 2003. Denitrification at low temperatures using a suspended carrier biofilm process. Water Res. 37 (10), 2394–2398.
Wilson, T., Toth, Z., Anderson, G., McSweeny, R., McGettigan, J., 2008. Using MBBRs to meet ENR nitrogen levels for over 8 years. Proceedings of the Water Environment Federation, WEFTEC 2008. Chicago, USA. Oct. 18–22.

Editorial Board of Journal of Environmental Sciences

JOURNAL OF ENVIRONMENTAL SCIENCES

环境科学学报(英文版)

www.jesc.ac.cn

Aims and scope

Journal of Environmental Sciences is an international academic journal supervised by Research Center for Eco-Environmental Sciences, Chinese Academy of Sciences. The journal publishes original, peer-reviewed innovative research and valuable findings in environmental sciences. The types of articles published are research article, critical review, rapid communications, and special issues.

The scope of the journal embraces the treatment processes for natural groundwater, municipal, agricultural and industrial water and wastewaters; physical and chemical methods for limitation of pollutants emission into the atmospheric environment; chemical and biological and phytoremediation of contaminated soil; fate and transport of pollutants in environments; toxicological effects of terrorist chemical release on the natural environment and human health; development of environmental catalysts and materials.

For subscription to electronic edition

Elsevier is responsible for subscription of the journal. Please subscribe to the journal via http://www.elsevier.com/locate/jes.

For subscription to print edition

China: Please contact the customer service, Science Press, 16 Donghuangchenggen North Street, Beijing 100717, China. Tel: +86-10-64017032; E-mail: journal@mail.sciencep.com, or the local post office throughout China (domestic postcode: 2-580).

Outside China: Please order the journal from the Elsevier Customer Service Department at the Regional Sales Office nearest you.

Submission declaration

Submission of the work described has not been published previously (except in the form of an abstract or as part of a published lecture or academic thesis), that it is not under consideration for publication elsewhere. The publication should be approved by all authors and tacitly or explicitly by the responsible authorities where the work was carried out. If the manuscript accepted, it will not be published elsewhere in the same form, in English or in any other language, including electronically without the written consent of the copyright-holder.

Editorial

Authors should submit manuscript online at http://www.jesc.ac.cn. In case of queries, please contact editorial office, Tel: +86-10-62920553, E-mail: jesc@rcees.ac.cn. Instruction to authors is available at http://www.jesc.ac.cn.

Journal of Environmental Sciences (Established in 1989)
Volume 32 2015

Supervised by	Chinese Academy of Sciences	**Published by**	Science Press, Beijing, China
Sponsored by	Research Center for Eco-Environmental		Elsevier Limited, The Netherlands
	Sciences, Chinese Academy of Sciences	**Distributed by**	
Edited by	Editorial Office of Journal of	Domestic	Science Press, 16 Donghuangchenggen
	Environmental Sciences		North Street, Beijing 100717, China
	P. O. Box 2871, Beijing 100085, China		Local Post Offices through China
	Tel: 86-10-62920553; http://www.jesc.ac.cn	Foreign	Elsevier Limited
	E-mail: jesc@rcees.ac.cn		http://www.elsevier.com/locate/jes
Editor-in-chief	X. Chris Le	**Printed by**	Beijing Beilin Printing House, 100083, China

CN 11-2629/X **Domestic postcode: 2-580** **Domestic price per issue RMB ¥ 110.00**

ISSN 1001-0742